

Mechanical stabilisation of austenite

S. Chatterjee¹, H.-S. Wang², J. R. Yang² and H. K. D. H. Bhadeshia*¹

A theory has been developed for the mechanical stabilisation of plastically deformed austenite by balancing the force which drives the transformation interface against the resistance from dislocation debris in the austenite. The work has been used to explain why very large strains are required to mechanically stabilise certain stainless steels, and also to interpret the subunit mechanism of bainite growth.

Keywords: Mechanical stabilisation, Martensite, Bainite, Austenitic stainless steels, Dislocations

Introduction

Displacive transformations involve the coordinated movement of atoms. Such movements cannot be sustained against strong defects such as grain boundaries. This is why martensite plates are unable to cross grain boundaries. Less drastic defects such as isolated dislocations also hinder the progress of such transformations, but can often be incorporated into the martensite lattice. However, it is well established¹⁻⁷ that when the strain in the austenite becomes sufficiently large, the motion of glissile interfaces becomes impossible, causing the transformation to halt.

This applies to all cases involving the translation of glissile interfaces, whether their motion leads to a phase change,¹⁻¹⁸ or simply to a reorientation of the lattice as in mechanical twinning.¹⁹ The phenomenon is known as mechanical stabilisation and is a sure way of distinguishing the displacive and reconstructive mechanisms of solid state transformations.²⁰

The primary purpose of the present work was to express the phenomenon of mechanical stabilisation into a theoretical framework capable of predicting the strain required to initiate stabilisation. The problem is one of dislocation interactions since a glissile transformation interface has a dislocation structure which has to move through any obstacles that exist in the austenite.

Method

A theory for predicting the onset of mechanical stabilisation is developed here by balancing the force which drives the motion of the interface against the resistance of the dislocation debris created by the deformation of the austenite.

Deformation at low homologous temperatures is produced by the translation of dislocations. For a density ρ of dislocations, each with a Burgers vector of

magnitude b , the plastic strain is given by

$$\varepsilon = \rho b L \quad (1)$$

where L is the average distance moved by the dislocations.²¹ For a given dislocation density, the spacing between the dislocations is given by $l = \rho^{-1/2}$. The mean shear stress τ needed to force dislocations past each other is, in these circumstances²¹

$$\tau = \frac{Gb}{8\pi(1-\nu)l} = \frac{Gb\rho^{1/2}}{8\pi(1-\nu)} \quad (2)$$

where G is the shear modulus and ν the Poisson's ratio. On combining with equation (1) and noting that the force per unit length is τb

$$\tau b = \frac{Gb^{3/2}}{8\pi(1-\nu)} \left(\frac{\varepsilon}{L}\right)^{1/2} \quad (3)$$

the mean free distance L must decrease as the plastic strain increases²²

$$L = \frac{\delta D}{\delta + D\varepsilon} \quad (4)$$

where D is the original grain size of austenite before straining and δ is a coefficient equal to $\sim 1 \mu\text{m}$ (Ref. 22).

Apart from dislocation strengthening, solid solution hardening will also contribute to the resistance to interface motion.^{23,24} Solid solution hardening coefficients for a variety of solutes in austenite have been reported for tensile strength²⁵ and were converted into shear stress equivalents τ_S using the Tresca criterion. This adds to the resistance owing to any dislocation debris.

Chemical driving force

The stress τ_T driving the motion of the interface originates from the chemical free energy change ΔG of transformation²³

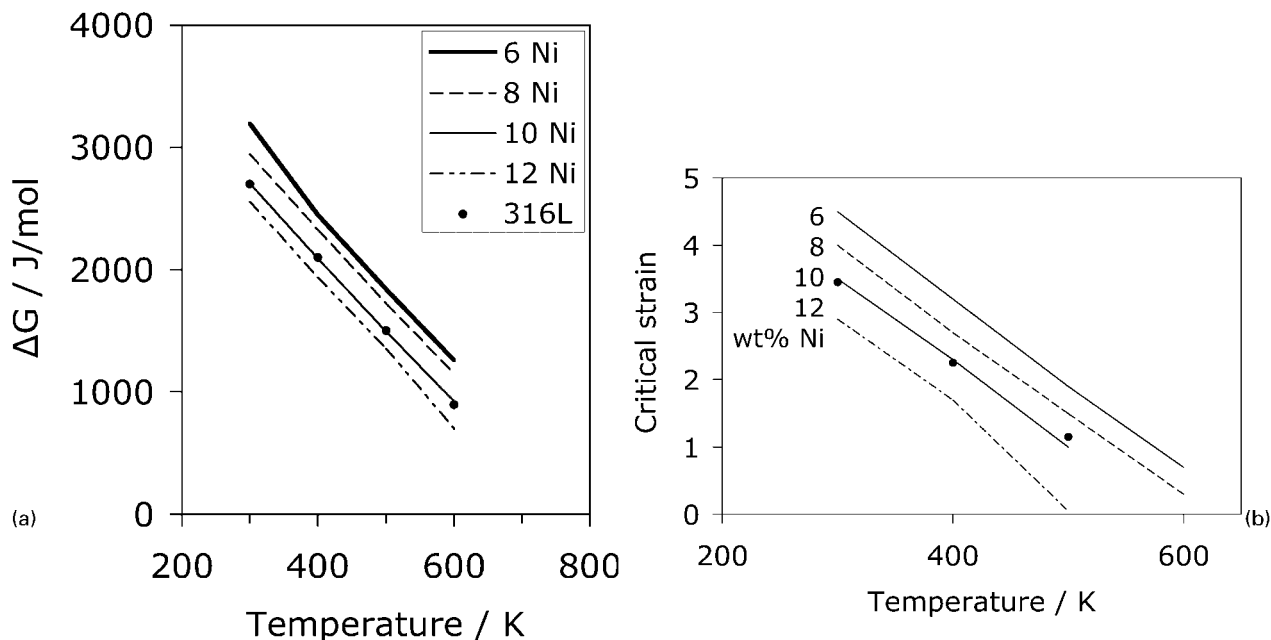
$$\tau_T = \phi \Delta G \quad (5)$$

where ϕ is a constant assumed to be equal to unity and $\Delta G = G_\gamma - G_\alpha$, i.e. the magnitude of the driving force. ΔG is a function of temperature and the composition of the steel – it was calculated using the

¹University of Cambridge, Materials Science and Metallurgy Pembroke Street, Cambridge CB2 3QZ, UK

²National Taiwan University Materials Science and Engineering, 1 Roosevelt Road, Section 4, Taipei 106, Taiwan

*Corresponding author, email hkdb@cus.cam.ac.uk



a variation in ΔG as function of alloy and temperature; b critical values of plastic strain for mechanical stabilisation of austenite

1 Lines represent alloys 1–4 and points alloy 316L

software MTDATA, which accesses thermodynamic data (SGTE database) to calculate phase stabilities and free energies. The stored energy of martensite is $\sim 600 \text{ J mol}^{-1}$ (Ref. 27) and that for bainite is $\sim 400 \text{ J mol}^{-1}$ (Ref. 28), values which were subtracted from the calculations obtained using MTDATA. When multiplied by Burger’s vector b , this gives the magnitude of force per unit length available for the austenite/martensite interface to move.

Mechanical stabilisation occurs when the stress driving the interface equals that opposing its motion

$$\tau_T = \tau + \tau_S$$

$$b\Delta G = \frac{1}{8\pi(1-\nu)} Gb^{3/2} \left(\frac{\epsilon}{L}\right)^{1/2} + \tau_S b \quad (6)$$

this equation can now be used to calculate the critical strain for mechanical stabilisation.

Results and discussion

All calculations were carried out using the data listed in Table 1, beginning with austenitic stainless steels alloys 1–4 as listed in Table 2. The reason for varying the nickel concentration was to study the effect of the chemical driving force for transformation on the stabilisation to martensitic transformation. All the calculations were carried out allowing for solid solution strengthening and for a variety of temperatures.

Table 1 Values of inputs in calculations

Property	Value
Shear modulus of austenite, Pa	8×10^{10}
Poisson’s ratio	0.27
Burgers vector, m	2.52×10^{-10}
δ , m	10^{-6}
Grain size, m	4×10^{-5}

Austenitic stainless steels

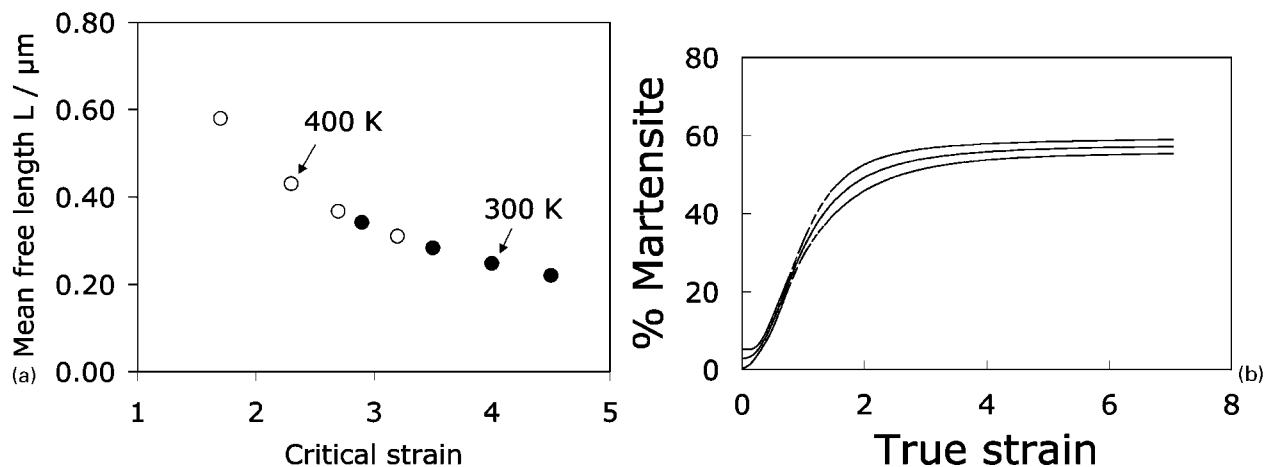
Figure 1a shows the chemical driving force (before the subtraction of 600 J mol^{-1} stored energy) as calculated using MTDATA. It is seen that these are very large driving forces, especially for 300 K which is normally the ambient deformation temperature. It is therefore not surprising that the critical strain ϵ calculated using equation (6) is large, ranging from 2.9–4.5, the larger value corresponding to the smallest nickel concentration, i.e. the largest ΔG , as shown in Fig. 1b.

In physical terms, this means that the mean free path L has to be very small $< 1 \mu\text{m}$, as illustrated in Fig. 2. Huge plastic strains are required to achieve the necessary defect density so such a result may at first sight seem unlikely. However, recent work on 316L austenitic stainless steel deformed to a true strain of $\epsilon = 6.3$ confirms that severe deformation is indeed necessary to mechanically stabilise the austenite.²⁹

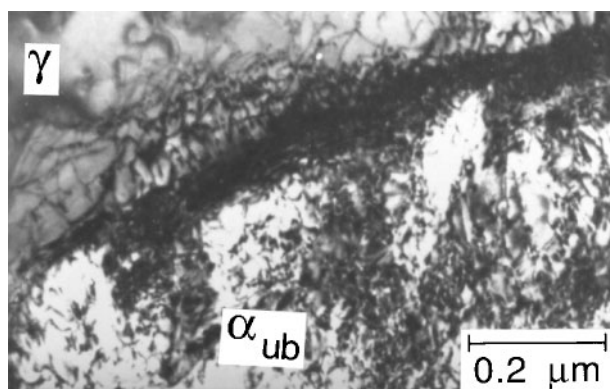
Figure 2b shows the curve obtained by fitting to experimental data from the 316L experiments.²⁹ It was demonstrated in the same work that on the basis of the thermodynamics, the alloy should be able to transform completely into martensite, were it not for the fact that the deformed austenite becomes mechanically stabilised. In fact, the amount of strain induced martensite achievable is limited to 57%, much of this forming at low strains before the onset of stabilisation. On the basis of the fitted curve (Fig. 2b), the onset of mechanical stabilisation, i.e. the strain at which strain induced

Table 2 Chemical compositions in wt-%

Alloy	C	Mn	Si	Cr	Ni	Mo	N
Alloy 1	0.05	1.5	0.75	18.0	6.0	0.0	0.03
Alloy 2	0.05	1.5	0.75	18.0	8.0	0.0	0.03
Alloy 3	0.05	1.5	0.75	18.0	10.0	0.0	0.03
Alloy 4	0.05	1.5	0.75	18.0	12.0	0.0	0.03
316 L	0.01	0.53	0.75	17.1	11.9	2.0	
Bainitic	0.4	3.0	2.0				



2 a mean free path at point where mechanical stabilisation occurs as function of temperature and nickel concentration: each set of points represents alloys 1–4, lowest Ni concentration corresponding to smallest L in each set and b fraction of martensite as function of strain in 316L: bounding curves represent $\pm 1\sigma$ uncertainties in modelling experimental data²⁹



3 Intense dislocation debris at and in vicinity of bainite (α_{ub})/austenite (γ) interface:³² steel has chemical composition Fe–0.43C–3Mn–2.12Si (wt-%) and is transformed at 350°C (623K)

martensite ceases, is about $\varepsilon \approx 2 \rightarrow 3$. The calculated data for 316L are presented as points in Fig. 1b; they show that the critical strain for mechanical stabilisation is 3.45, 2.25 and 1.45 for the temperatures 300, 400 and 500 K respectively. The large strain data of the experiments²⁹ are based on wire drawing and it is conceivable that the temperature rises by ~ 200 K during the deformation.³⁰ The calculations are therefore judged to be consistent with the experimental data. Furthermore, the analysis shows that the reason why such large strains are needed to achieve stabilisation is the large values of ΔG associated with such stainless steels at the deformation temperature.

Bainitic steels

One of the fascinating aspects of the bainite reaction in steels is that it occurs by a subunit mechanism in which a platelet of ferrite grows to a limited size even though

Table 3 Data for Fe–Mn–Si–C steel

Temperature, K	Critical strain
500	2.1
600	0.6
650	0.06

there is no impingement with obstacles such as austenite grain boundaries. The transformation then propagates by the nucleation and growth of another subunit, the collection of subunits being known as a sheaf.³¹ The reason why each platelet only grows to a limited size is that the shape deformation accompanying transformation is plastically accommodated in the austenite beside the plate.³² This results in the creation of an intense dislocation debris which renders the interface immobile, as illustrated in Fig. 3.

Calculations were therefore carried out for the bainitic steel listed in Table 2, which is also the steel from which the micrograph in Fig. 3 originates, for a transformation temperature of 623 K. As pointed out previously, the stored energy used was 400 J mol^{-1} . The results are presented in Table 3. The shear strain associated with the growth of bainite is ~ 0.26 (Ref. 33) which on comparison with the calculated data, is sufficient to generate local mechanical stabilisation, and hence a subunit mechanism of growth. Furthermore, the length of the subunit is expected to become larger as this is qualitatively consistent with experimental data on bainite that the plates become more slender as the transformation temperature is reduced (ΔG increased).¹⁸ Note that martensite forms in this steel below ~ 500 K (Ref. 32).

Summary

A theory has been developed for the mechanical stabilisation of plastically deformed austenite by balancing the force which drives the transformation interface against the resistance from dislocation debris in the austenite. The key input to the model includes the chemical free energy accompanying the transformation and the transformation temperature.

The theory seems to explain why very large strains are required to mechanically stabilise certain stainless steels and provides a rationale for the subunit mechanism of bainite growth.

Acknowledgements

The authors are grateful to Tata Steel (India), the National Science Foundation (Taiwan) and the Royal Society (UK) for funding this research.

References

1. H. K. D. H. Bhadeshia: *Mater. Sci. Eng. A*, 1999, **A273–275**, 58–66.
2. E. S. Machlin and M. Cohen: *Trans. AIME*, 1951, **191**, 746–754.
3. H. C. Fiedler, B. L. Averbach and M. Cohen: *Trans. ASM*, 1955, **47**, 267–290.
4. W. C. Leslie and R. L. Miller: *ASM Trans. Q.*, 1964, **57**, 972–979.
5. J. R. Strife, M. J. Carr and G. S. Ansell: *Metall. Trans. A*, 1976, **8A**, 1471–1484.
6. V. Raghavan: 'Martensite, a tribute to Morris Cohen', (ed. G. B. Olson and W. S. Owen), 197–226; 1992, Materials Park, OH, ASM International.
7. K. Tsuzaki, S. Fukasaku, Y. Tomota and T. Maki: *Mater. Trans. JIM*, 1991, **32**, 222–228.
8. J. F. Breedis and W. D. Robertson: *Acta Metall.*, 1963, **11**, 547–559.
9. R. Lagneborg: *Acta Metall.*, 1964, **12**, 823–843.
10. J. R. C. Guimares and J. C. Gomes: *Mater. Sci. Eng.*, 1979, **39**, 187–191.
11. Ch. Maier, O. Blaschko and W. Pichl: *Phys. Rev. B*, 1995, **B52**, 9283–9290.
12. J. R. Yang, C. Y. Huang, W. H. Hsieh and C. S. Chiou: *Mater. Trans. JIM*, 1996, **37**, 579–585.
13. X. Song, N. Gu and H. Peng: *Defect Diffus. Forum*, 1997, **148–149**, 165–167.
14. M. C. Tsai, C. S. Chiou, J. S. Du and J. R. Yang: *Mater. Sci. Eng. A*, 2002, **A332**, 1–10.
15. P. H. Shipway and H. K. D. H. Bhadeshia: *Mater. Sci. Eng. A*, 1997, **A223**, 179–186.
16. J. R. Yang and L. C. Chang: *Mater. Sci. Eng. A*, 1997, **A223**, 158–167.
17. P. H. Shipway and H. K. D. H. Bhadeshia: *Mater. Sci. Technol.*, 1995, **11**, 1116–1128.
18. S. B. Singh and H. K. D. H. Bhadeshia: *Mater. Sci. Technol.*, 1996, **12**, 610–612.
19. J. W. Christian and S. Mahajan: *Prog. Mater. Sci.*, 1995, **39**, 1–157.
20. H. K. D. H. Bhadeshia: *Mater. Sci. Eng. A*, 2004, **378A**, 34–39.
21. R. W. K. Honeycombe: 'Plastic deformation of metals', 2nd edn; 1984, London, Edward Arnold.
22. F. Barlat, M. V. Glazov, J. C. Brem and D. J. Lege: *Int. J. Plasticity*, 2002, **18**, 919–939.
23. Olson, G. B. and M. Cohen: *Metall. Trans. A*, 1976, **7A**, 1897–1923.
24. G. Ghosh and G. B. Olson: *J. Phase Equilib.*, 2001, **22**, 199–207.
25. K. J. Irvine, T. Gladman and F. B. Pickering: *J. Iron Steel Inst.*, 1969, **207**, 1017–1028.
26. MTDATA, National Physical Laboratory, Teddington, London, 2005.
27. J. W. Christian: Proc. Int. Conf. ICOMAT 79, Boston, MA, USA, June 1979, MIT Press, 220–234.
28. H. K. D. H. Bhadeshia: *Acta Metall.*, 1981, **29**, 1117–1130.
29. H.-S. Wang, J. R. Yang and H. K. D. H. Bhadeshia: *Mater. Sci. Technol.*, 2005, **21**, 1323–1328.
30. J. R. Yang: Private communication, 2005.
31. R. F. Hehemann: 'Phase transformations', 397–432; 1970, Materials Park, OH, USA, ASM.
32. H. K. D. H. Bhadeshia and D. V. Edmonds: *Metall. Trans. A*, 1979, **10A**, 895–907.
33. E. Swallow and H. K. D. H. Bhadeshia: *Mater. Sci. Technol.*, 1996, **12**, 121–125.